Fermilab Library
0 1160 0039168 4
LYCEN-9430
FERMILAB
AUG 1 19
18

LYCEN/9430
Juillet 1994

DO WE SEE THE SAME POMERON IN ELASTIC AND DEEP INELASTIC SCATTERING ?

M. Bertini and M. Giffon

Institut de Physique Nucléaire de Lyon, IN2P3-CNRS et Université Claude Bernard
43 boulevard du 11 Novembre 1918, F-69622 Villeurbanne Cedex, France

L. Jenkovszky

Institut for Theoretical Physics
Kiev-143, Ukraine

Abstract

A model for the proton structure function (SF) including various features expected from the theory - both of perturbative QCD and non-perturbative (Regge) theory - is constructed. Good agreement whith data on deep inelastic scattering and photoproduction data is in the case when the non-perturbative component of the Pomeron is governed by a "maxinal" behaviour, i.e. the one growing like $\log^2(s)$.

Submitted to Zeitschrift f. Physik C

NAME	I D No.	

RETURN TO FERMILAB LIBRARY

1 - Introduction

The recent experimental data from HERA opened a new area in the study of proton structure function (SF) $F_2(x, Q^2)$. The available data now cover a wide kinematic range linking the perturbative and non-perturbative regimes expected in QCD.

In fact, the H1 [1] and ZEUS [2] collaboration, present results for F_2 at very small-x ($x < 10^{-3}$) which offer the opportunity to probe the perturbative role of the Pomeron which is expected to govern the small-x and large-Q^2 behaviour of F_2. The results [3,4] of these collaborations for the total (γp) cross section ($\sigma_{tot}^{\gamma p}$) at high energy ($\sqrt{s} \approx 200$ GeV) lead to a similar situation because in this energy range, it is the so called non-perturbative Pomeron which, as expected from Regge theory, is the dominant contribution.

The nature of the Pomeron remains among the unsolved problems of QCD. It became popular [5] to treat the Pomeron as a dual object, "soft" or "hard" depending on the kinematical region considered.

The link between deep inelastic scattering (DIS) and elastic hadron scattering has been studied in a number of papers (see e.g [5-8]). Donnachie-Landshoff used [7] their model of the Pomeron with the intercept $\alpha(0)$ ($\alpha(0) \sim 1.08$) fitted earlier to the hadronic reactions to describe the small-Q^2 behaviour of the structure function. By introducing in a phenomenological way some Q^2 dependence in the Pomeron intercept, and combining it with the generalized eikonal model, in Ref.[8] good agreement with the data has been obtained in a wide range of Q^2.

In this paper we combine the small-Q^2 behaviour of the Pomeron with its Q^2 evolution deduced from the Gribov-Lipatov-Altarelli-Parisi (GLAP) equations. Following the Lopez and Indurain arguments [9] we investigate the large-Q^2 behaviour of SF closed to $x = 0$ and $x = 1$, keeping in the GLAP equations the leading contributions. In the low Q^2 domain, we assume that the behaviour of SF is governed by non-perturbative contribution, consequently, only this contributions have to be extented to Q^2=0. The small-Q^2 parametrization of SF is deduced from results on γp and hadronic cross sections. Various models for the non-perturbative Pomeron contribution will be tested.

In section 2 we present our model and the derivation of the main formulae to be used in what follows. In section 3 we confront the model against the experimental data and present some conclusions.

2 - The model

Following the ideas presented in the introduction, we write the structure function F_2 as a sum of two terms :

$$F_2 = F_2{}^{npert} + F_2{}^{pert} \ , \tag{1}$$

where the first term, F_2^{npert} , corresponds to the non-perturbative part of the structure function, typical of the small-Q^2 behaviour and the second one, F_2^{pert} , to the perturbative large-Q^2 evolution. In what follows, F_2^{npert} will be connected with Regge behaviour and in particular it will be chosen to describe $\sigma_{tot}^{\gamma p}$ [10,11], while F_2^{pert} will be derived from the asymptotically large-Q^2 solutions of GLAP equations [12,13].

As it is well known [14] the total γp photoproduction cross section can be described by the exchange of a Pomeron and a Reggeon term :

$$\sigma_{tot}^{\gamma p} = \sigma(Pomeron) + \sigma(Reggeon) \ . \tag{2}$$

We extend this form to include deep inelastic scattering by assuming that the Pomeron is related to the sea and gluon (singlet) distribution, dominating the small-x behaviour, while the reggeons are related to the valence quark (nonsinglet) distribution, important at large-x.

Now, each term F_2^i ($i = pert, npert$) of F_2 can be written as a sum [6] :

$$F_2{}^i(x, Q^2) = xP^i(x, Q^2) + xV^i(x, Q^2) \ , \tag{3}$$

where $P(x, Q^2)$ is the singlet distribution mainly responsible for the small-x behaviour of F_2, and $V(x, Q^2)$ the non singlet distribution responsible for the large-x behaviour.

2.1 Determination of F_2^{pert}

Both contributions in F_2^{pert} are defined at moderatly large value of $Q^2 = Q_0^2$, where perturbative hypothesis are expected to be valid, and then evolved via GLAP equations. We chose $Q_0^2 = 5$ GeV^2 in agreement with the often used value [15].

Since the sea and gluons content of the proton is closely related to the Pomeron, one must impose, in its input distribution at $Q^2 = Q_0^2$, the steep behaviour (in $x^{-\lambda}$) predicted by the Lipatov equation [13] as x goes to 0. Then, the small-x behaviour of the Pomeron at $Q^2 = Q_0^2$ is given by :

$$xP^{pert}(x, Q_0^2) \xrightarrow[x \to 0]{} A_p \ x^{-\delta_p} \ . \tag{4}$$

Following [16], we choose to work in the pure gluon sector of QCD since it is the gluons which are expected to drive the small-x behaviour and use the relevant GLAP evolution equation for gluons similarly to the method using in [17] :

$$\frac{d\left(xP^{pert}(x, Q^2)\right)}{d\ s} \approx x \int_x^1 \frac{dy}{y^2} \ P_{gg}(\frac{x}{y}) \ y \ P^{pert}(y, Q^2) \ , \tag{5}$$

with

$$s = \log \left(\frac{\log Q^2/\Lambda^2}{\log Q_0^2/\Lambda^2}\right) \ .$$

By writting the running coupling constant in the leading order approximation :

$$\alpha_s(Q^2) = \frac{4\pi}{\beta_0 \log\ (Q^2/\Lambda^2)} \ ,$$

with $\beta_0 = (11N_c - 2N_f)/3$, and choosing $\Lambda = 200$ MeV, $N_c = 3$ and $N_f = 4$, then the gg kernel is given by :

$$P_{gg}(z) = \frac{2}{\beta_0}\left[2N_c\left(\left(\frac{z}{1-z}\right)_+ + \frac{1-z}{z} + z(1-z)\right) + \beta_0\delta(1-z)\right] . \tag{6}$$

Following [18], we now evaluate the integral in (5) with (4) and compare the result with the relevant derivative in s. In this way we obtain the evolution with s of the coefficient A_p in (4) :

$$A_p(s) = A_p \exp(d_{gg}s) ,$$

with :

$$d_{gg}(\delta_P) = \frac{2}{\beta_0}\left[2N_c\left(\frac{11}{12} + \frac{1-\delta_p}{\delta_p(\delta_p+1)} + \frac{1}{(\delta_p+2)(\delta_p+3)} - \left(\Psi(\delta_p+1)+\gamma\right)\right) - \frac{N_f}{3}\right] , \tag{7}$$

where Ψ is the logarithmic derivative of the Euler gamma function, and γ is the Euler's constant. The evolution of the δ_p parameter cannot be obtained in this way since it is the eigenvalue of the kernel P_{gg}. We shall find it from fits to the data.

Even though the Pomeron dominates the small-x region, its contribution at intermediate and large x is still non-negligible. This will be taken into account by relevant multipliers by which (4) becomes :

$$xP^{pert}(x,Q^2) = A_p\ e^{d_{gg}(\delta_p)s}\ x^{-\delta_p}(1+\epsilon_p x)(1-x)^{\beta_p} , \tag{8}$$

where, the last two factors in Eq.(8) reflect respectively the contribution in the intermediate and large-x region.

For the valence term, which is increasingly important for x close to 1, we can write this non singlet distribution at $Q^2 = Q_0^2$:

$$xV^{pert}(x,Q_0^2) \xrightarrow[x\to 1]{} A_v(1-x)^{\beta_v} . \tag{9}$$

The relevant GLAP equation is :

$$\frac{d\ \left(xV^{pert}(x,Q^2)\right)}{d\ s} = x\int_x^1 \frac{dy}{y^2}\ P_{qq}(\frac{x}{y})\ y\ V^{pert}(y,Q^2) , \tag{10}$$

where using the same evolution variable and parameters as in Eq.(5) the qq kernel is :

$$P_{qq}(z) = \frac{2C_f}{\beta_0}\left[\left(\frac{1+z^2}{1-z}\right)_+ + \frac{3}{2}\delta(1-z)\right] , \tag{11}$$

with $C_f = (N_c^2-1)/2N_c$. By proceeding in the similar way as above we find the evolution of β_v and A_v :

$$A_v(s) = A_v e^{(\rho s)}\frac{\Gamma(\beta_v+1)}{\Gamma(\beta_v(s)+1)}$$

$$\beta_v(s) = \beta_v + \frac{4C_f}{\beta_0}s ,$$

where :

$$\rho = \frac{4C_f}{\beta_0}(\frac{3}{4} - \gamma) \ .$$

To take into account the small-x contribution for the valence quark distribution we include phenomenological multipliers (as above) whereafter the non-singlet distribution becomes :

$$xV^{pert}(x, Q^2) = A_v e^{\rho s} \frac{\Gamma(\beta_v + 1)}{\Gamma(\beta_v(s) + 1)} \ x^{-\delta_v}(1 + h_0\sqrt{x} + h_1 x)(1 - x)^{\beta_v(s)} \ , \qquad (12)$$

where $(1 + h_0\sqrt{x} + h_1 x)$ and $x^{-\delta_v}$ $(\delta_v < 0)$ are introduced to describe respectively the intermediate x-region and the flavor Regge behaviour for small-x.

2.2 Small-Q^2 contribution and extention to $Q^2 = 0$.

We now consider the small-Q^2 behaviour of F_2 and the possible extension to $Q^2 = 0$. A major problem is that one does not know exactly the transition region between the perturbative and non-perturbative dynamics. The lowest value of Q^2 from which evolution starts can only be guessed (we have assumed $Q_0^2 = 5$ GeV^2 but alternative value are not excluded). The interpolation between the two regimes is a challenge for the theory.

As a guide, we choose F_2 to be compatible with the photoproduction total cross-section $\sigma_{tot}^{\gamma p}$.

We also impose the requirement of gauge invariance that the structure function F_2 vanishes like Q^2 as $Q^2 \to 0$. Correspondingly, to fulfill the above requirement, we extend at least in an approximative way, the analytical expressions (8) and (12) of F_2^{pert} by changing the exponential factors into a power behaviour (see also [7]). The modified perturbative components of the structure function (8) and (12) thus become :

$$xP^{pert}(x, Q^2) = B_p \Phi_p(Q^2) \ x^{-\delta_p}(1 + \epsilon_p x)(1 - x)^{\beta_p} \qquad (13)$$

$$xV^{pert}(x, Q^2) = B_v \Phi_v(Q^2) \frac{\Gamma(\beta_v + 1)}{\Gamma(\beta_v(t) + 1)} \ x^{-\delta_v}(1 + h_0\sqrt{x} + h_1 x)(1 - x)^{\beta_v(t)} \ , \qquad (14)$$

where we have "frozen" the infrared divergence in the evolution by using :

$$t = \log \left(\frac{\log(Q^2 + Q_0^2)/2\Lambda^2}{\log Q_0^2/\Lambda^2} \right) \ .$$

The Φ_i functions for $i = p, v$ are defined as :

$$\Phi_i = \left(\frac{Q^2/Q_0^2}{Q^2/Q_0^2 + b_i^2} \right)^{(1+\delta_i)} \ , \qquad (15)$$

where the parameters b_i^2 can be related to the radius of the i parton form factor of the proton.

In formulae (13-15) the coefficients B_i and b_i in (13-15) as well as the t-dependence $\beta_v(t)$ in (14) are expressed in terms of δ_i and A_i in (8) and (12) by requiring respectively a smooth join between the two forms at $Q^2 = Q_0^2$.

Such an extension is quite acceptable in the small-Q^2 region but it is certainly not for Q^2=0 since it provides a "Lipatov" behaviour for the total cross-section which has not been confirmed by the data (see e.g [7,11]). To fit the observed behaviour of $\sigma_{tot}^{\gamma p}$, we thus assume that the behaviour at Q^2=0 is completely yielded by the non-perturbative contribution F_2^{npert} in Eq.(1).

Thus for small and vanishing Q^2, F_2 in Eq.(1) becomes :

$$F_2 = \left[\frac{Q_0^2}{Q^2+Q_0^2}\right]^{\nu_{npert}} F_2{}^{npert} + \left[\frac{Q^2}{Q^2+Q_0^2}\right]^{\nu_{pert}} F_2{}^{pert} , \tag{16}$$

where the ν_i is an adjustable parameter to provide the smooth interpolation between the two regimes.

According to the additivity of various Regge contributions, as discussed in the introduction, we write F_2^{npert} as a sum of two terms :

$$F_2^{npert} = F_{2\,Pomeron}^{npert} + F_{2\,Reggeon}^{npert} , \tag{17}$$

where the fulfilment of the above requirements is implied.

Two different type of Pomeron will be used :

i) a "Froissart" like Pomeron :

$$F_{2\,Pomeron}^{npert} = (c_3 + c_2 L + c_1 L^2)(1-x)^b \log\left(1 + \frac{Q^2}{Q^2+c_0^2}\right) , \tag{18}$$

where $L = \log\left((Q^2(1/x-1)+m_N^2\right)$, m_N being the proton mass; in this first case two options will be considered, that of a maximal (as L^2) and a moderate (as L, $c_1 = 0$) growth [11], and,

ii) a supercritical Pomeron [10] :

$$F_{2\,Pomeron}^{npert} = d_1\left(\frac{Q^2}{Q^2+d_0^2}\right)^{1+\varepsilon} x^{-\varepsilon}(1-x)^{d_2} , \tag{19}$$

with $\varepsilon > 0$. The secondary Reggeon term is chosen as (with $\delta_R < 0$),

$$F_{2\,Reggeon}^{npert} = a_R\left(\frac{Q^2}{Q^2+a_0^2}\right)^{1+\delta_R} x^{-\delta_R}(1-x)^{\beta_R} . \tag{20}$$

From the definition of the total cross section $\sigma_{tot}^{\gamma p}$:

$$\sigma_{tot}^{\gamma p} = \lim_{Q^2\to 0}\left[\frac{4\pi^2\alpha_{EM}}{Q^2}F_2(x,Q^2)\right] , \tag{21}$$

we thus have for the two above models of the Pomeron :

$$\sigma_{tot}^{\gamma p} \alpha\, a_R \left(\frac{1}{a_0^2}\right)^{1+\delta_R} s^{\delta_R} + \frac{1}{c_0^2}\left(c_3 + c_2 \log(s) + c_1 \log^2(s)\right) , \tag{22}$$

and

$$\sigma_{tot}^{\gamma p} \alpha\, a_R \left(\frac{1}{a_0^2}\right)^{1+\delta_R} s^{\delta_R} + d_1 \left(\frac{1}{d_0^2}\right)^{1+\epsilon} s^{\epsilon} . \tag{23}$$

3 - Results and conclusions.

The model of the proton structure function F_2 presented in the preceding sections was fitted in a wide kinematical range to a large number of experimental data on deep inelastic scattering from NMC [19], SLAC [20], BCDMS [21], H1 [1] and ZEUS [2], as well as those on photoproduction total cross-section $\sigma_{tot}^{\gamma p}$ from O.D Cadwell *et al.* [22], H1 [3], ZEUS [4].

To find the best choice, the fits were done separately for various models of the small-Q^2 component of the Pomeron presented in 2.2.

The fitting procedure proceeded in two step. First, we have fitted the parameters of the formulae (22) and (23) to the total cross-section ($\sigma_{tot}^{\gamma p}$) data. Then the remaining free parameters in F_2, (Eq. 15) were fitted to the data on deep inelastic scattering. The values of the parameters are presented in Table 1. One observation from these fits, shown in Figs.1 and Fig.2 is that, in agreement with the previous analyses of Ref.[15], the small-Q^2 behaviour of the SF has little influence on its large-Q^2 behaviour.

The next observation (see Fig.3) is that the small-x and large-Q^2 behaviour seems to be controlled by the so called "Lipatov Pomeron" (called also by Lopez and Indurain [9] the "singulariy of anomalous dimension"). This is pronounced as shown in Fig.4 where the respective role of the Pomeron contribution and the valence contribution is illustrated. The fitted value of δ_p was found close to 0.42 (see Table 1), which is in agreement with others works [15,23].

Our main conclusion is that two components of the Pomeron seems to be visible : one "moderate", fitting the γ-p total cross-section and the low-Q^2 data of SLAC, NMC, and BCDMS data, but inconsistent with the steep rise seen at HERA at small-x, and the other one, the QCD-inspired "Lipatov Pomeron", in agreement with the HERA increases of F_2 but implying a non realistic large-s rise of $\sigma_{tot}^{\gamma p}$. However, if we believe that there is one Pomeron, one way out is to introduce a Q^2-dependent of this intercept as done in Ref.[8].

The small-Q^2 behaviour of the structure function itself is informative in helping to resolve the long-standing problem of "how fast do cross sections rise"? The best fit to the total cross section (Fig.5) and low-Q^2 structure function (Fig.6) is achieved with a Froissaron-like Pomeron (i.e giving rise like $\log^2(s)$) rather than a slower (like $\log(s)$) or faster (s^{ϵ}) rise of energy, as founded in hadronic reactions [11].

In conclusion we have introduced a simple two-components model for the Pomeron, one component responsible for the small-Q^2 the other one for the large-Q^2 behaviour of the structure function. A large kinematical domain of F_2 and $\sigma_{tot}^{\gamma p}$ is well described by

our model. But evidently the complicated interplay of x and Q^2 dependence of SF is not completely understood. In the same way, the evolution of the Pomeron behaviour in the small-Q^2 to large-Q^2 deep inelastic process remains a debated problem.

We wish to thank X. Artru for enlightning discussions, and a critical reading of the manuscript.

References.

[1] I. Abt*et al.*, (H1 Collaboration) Phys. Lett. **B407** (1993) 515.

[2] M. Derrick *et al.*, (ZEUS Collaboration) Phys. Lett. **B316** (1993) 412.

[3] T. Ahmed *et al.*, (H1 Collaboration) Phys. Lett. **B299** (1993) 374.

[4] M. Derrick *et al.*, (ZEUS Collaboration) Phys. Lett. **B293** (1992) 465.

[5] See J.D. Bjorken Nucl. Phys. (Proc. Suppl.) **25B** (1992) 253, and references therein.

[6] H. Abramowicz, E.M. Levin, A. Levy, and U. Maor, Phys. lett. **B269** (1991) 465.

[7] A. Donnachie, and P.V. Landshoff, Z. Phys. **C61** (1994) 139.

[8] A. Capella, A. Kaidalov, C. Merini, and J. Tran Thanh Van, *Stucture functions and low X physics*, LPTHE Orsay 94-34, April 1994.

[9] C. Lopez and F.J. Indurain, Nucl. Phys. **B171** (1991) 231.

[10] A. Donnachie, and P.V. Landshoff, Phys. Lett. **B296** (1992) 227.

[11] P. Desgrolard, M. Giffon, A. Lengyel, and E. Martinov, Nuovo Cimento **A107** (1994) 637.

[12] G. Altarelli and G. Parisi, Nucl. Phys. **B126** (1977) 298;
G. Atarelli, Phys. Rep. 81 (1982) 1.
L.N. Lipatov, Sov. J. Nucl. Phys **20** (1975) 94.

[13] L. N. Lipatov Sov. Phys. JETP **63** (1986) 904;
L. N. Lipatov in *Perturbative QCD* , edited by A.H. Muller (World Scientific, Singapore, 1989)p. 411.

[14] G. Wolf, Proc. 1971 *Intern. Symp. on Electron and photon interactions at hight energies* (Cornell, 1971) p.85.

[15] A.D. Martin, W.J. Stirling and, R.G. Roberts, Phys. Rev **D47** (1993) 867; *MRS Partons Distributions* RAL-93-077.
J. Kwiecinsky, A.D. Martin, W.J. Stirling and, R.G. Roberts, Phys. Rev. **D42** (1990) 3645;
A. J. Askew, K. Golec-Biernat, J. Kwiecinsky, A.D. Martin, Phys. Lett. **B325** (1994) 218;
A. J. Askew, J . Kwiecinsky, A.D. Martin, P. J. Sutton Phys. Rev. **D49** (1994) 4402.

[16] J. C. Collins, J. Kwiecinski Nucl. Phys. **B316** (1989) 307.

[17] L. Jenkovszky, A.V. Kotikov, F. Paccanoni Phys. Lett. **B314** (1993) 421; Sov. J. Nucl. Phys. 55 (1992) 1224.
K. Prytz Phys. Lett. **B311** (1993) 286.

[18] A.V. Kotikov Phys. At. Nucl. **56** (1993) 1276;

M. Bertini, P. Desgrolard, M. Giffon, L. Jenkovszky, F. Paccanoni, *Phenomenological analysis of the small-x proton structure function* $F_2(x, Q^2)$, LYCEN 9366, December 1993.

[19] P. Amaudruz *et al.*, (NM Collaboration) Phys. Lett. **B295** (1992) 159.

[20] L.W. Whitlow *al.*, Phys. Lett **B282** (1992) 475; SLAC-Report-357 (March 1990).

[21] A.C. Benvenutti *et al.*, (BCDMS Collaboration) Phys. Lett. **B237** (1990) 599.

[22] D.O. Cadwell *et al.*, Phys. Rev. Lett 40 (1978) 1222; Phys. Rev. **D7** (1975) 1384; S.I. Alekhin *et al.* CERN-HERA 87-01 (1987).

[23] N.N. Nikolaev, B.G. Zakharov, Phys. Lett. **B327** (1994) 149.

Figures Captions

Fig.1.a,b. Comparison between the measurement of F_2 obtained from NMC [19] (closed points), SLAC [20] (squared dots), and BCDMS [21] (triangulated dots) and our parametrizations of stucture function. The continous, dotted, and dashed curves correspond to F_2 calculed with the common F_2^{pert} and respectively with the contribution F_2^{npert} parametrized as Eq.(18), Eq.(18) with $c_1 = 0$ (see the text), and Eq(19).

Fig.2. With the same definitions as for **Fig.1.a,b** the curves show the description of H1 [1] and ZEUS [2] measurements of F_2.

Fig.3. The structure function from H1 [1] (triangulated dots), ZEUS [2] (closed points) and NMC [19] (opened points), with the same tree parametrizations as for **Fig.1.**

Fig.4. Behaviour of the singlet and non-singlet distribution of F_2 at $Q^2 = 15$ GeV^2 with the same data defined in **Fig.3.**
The continuous line shows the description of the data defined in **Fig.3.** with our best parametrization (with F_2^{npert} taken as Eq.(18)). The dashed (dotted) curve, discribe the behaviour of the singlet (non-singlet) contribution of F_2.

Fig.5. Total cross section as a function of the γp center of mass energy W, with results from O.D. Caldwell [22] (closed points) , H1 [3] (opened square), ZEUS [4] (closed square and star). The dotted, continuous and dashed curves are obtained respectively from the parametrizations of Eq.(23), Eq.(22), and Eq.(22) with $c_1 = 0$ (see the text).

Fig.6. The structure function from NMC [19] at $Q^2 = 5$ GeV^2, with the same parametrizations as for **Fig.1**

	(a)	(b)	(c)	
c_1	$5.20\ 10^{-4}$	0.0		
c_2	$2.93\ 10^{-2}$	$5.07\ 10^{-2}$	0.192	d_1
c_3	0.220	0.347	$8.08\ 10^{-2}$	ϵ
c_0^2	0.428	0.662	0.346	d_0^2
a_R	$2.48\ 10^{-2}$	0.829	0.159	a_R
δ_R	-0.442	-0.488	-0.4525	δ_R
a_0^2	$8.85\ 10^{-4}$	0.389	$2.75\ 10^{-2}$	a_0^2
b	0.104	1.39	0.867	d_2
β_R	0.105	1.62	0.301	β_R
ν^{npert}	2.59	1.71	2.36	ν^{npert}

	(a)	(b)	(c)
A_p	$4.40\ 10^{-2}$	$3.53\ 10^{-2}$	$4.20\ 10^{-2}$
δ_p	0.408	0.438	0.432
ϵ_p	3.99	0.45	0.328
β_p	5.561	6.69	5.538
A_v	0.808	0.991	1.01
δ_v	-0.253	-0.11	-0.28
h_0	-1.19	-2.00	-1.23
h_1	5.12	6.43	4.52
β_v	3.50	3.80	3.56
ν^{pert}	0.382	1.40	0.523

Table 1

Value of parameters of $F_2(x, Q^2)$ obtained from fits to the data with Eq.(16).

The upper part of the table lists parameters involved in the small-Q^2 contribution (F_2^{npert}) of F_2 (parametrized as Eq.(17)), for the three different small-Q^2 behaviour of the Pomeron :(a) for Eq.(18), (b) for Eq.(18) (with $c_1 = 0$) and (c) for Eq.(19).
The lower part lists parameters involved in the large-Q^2 contribution (F_2^{pert}) of F_2 , parametrized with Eq.(8) and Eq.(12), for the three previously small-Q^2 parametrizations. The first seven parameters listed in the table are fixed from a fit to the total γp photoproduction cross section [3], [4], [22], and all others parameters are fitted to the all deep inelastic data [1], [2], [19], [20] , [21].

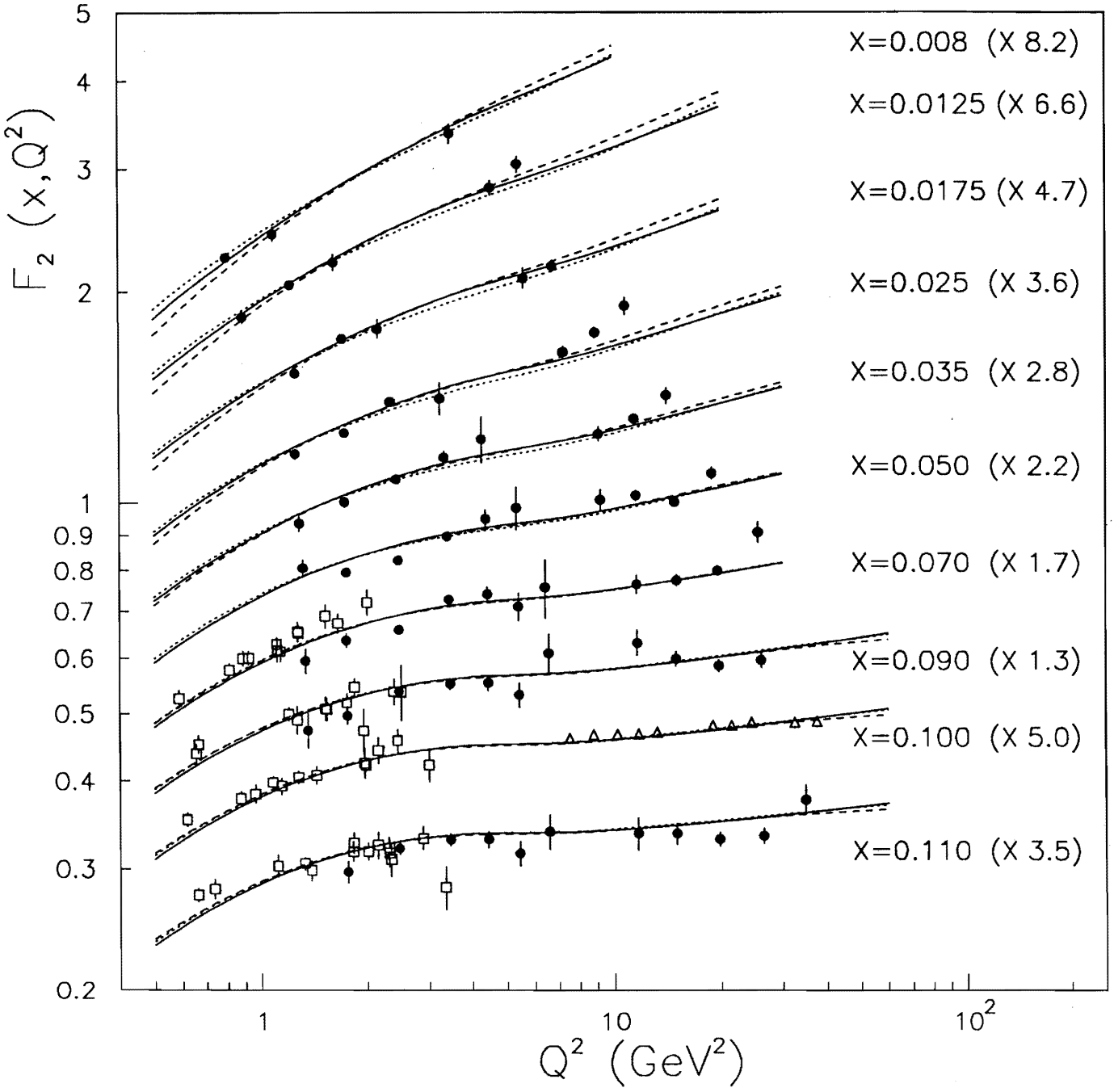
X=0.008 (X 8.2)
X=0.0125 (X 6.6)
X=0.0175 (X 4.7)
X=0.025 (X 3.6)
X=0.035 (X 2.8)
X=0.050 (X 2.2)
X=0.070 (X 1.7)
X=0.090 (X 1.3)
X=0.100 (X 5.0)
X=0.110 (X 3.5)
$F_2(x,Q^2)$
Q^2 (GeV^2)
5
4
3
2
1
0.9
0.8
0.7
0.6
0.5
0.4
0.3
0.2
1
10
10^2

Fig. 1.a

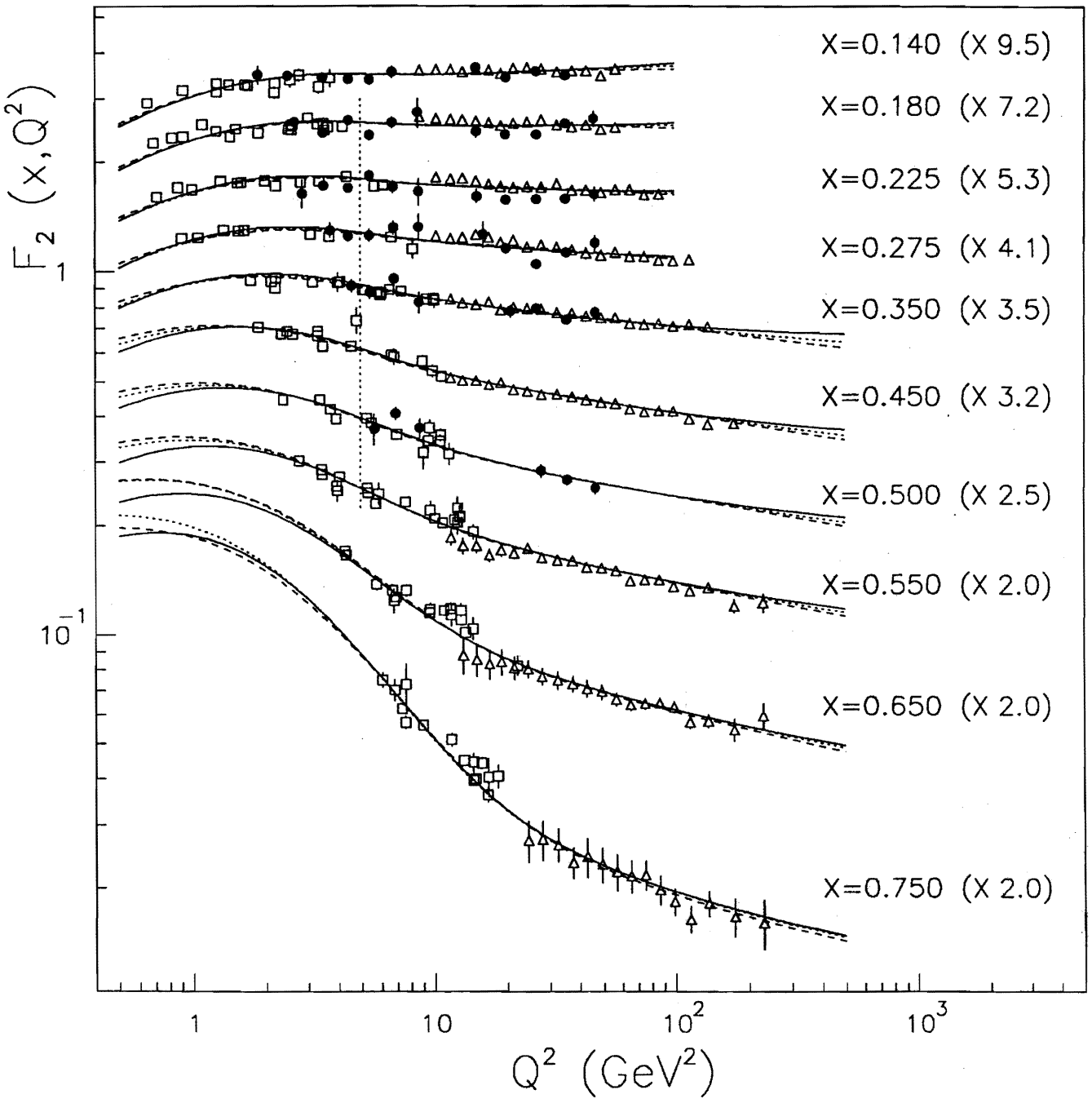
X=0.140 (X 9.5)
X=0.180 (X 7.2)
X=0.225 (X 5.3)
X=0.275 (X 4.1)
X=0.350 (X 3.5)
X=0.450 (X 3.2)
X=0.500 (X 2.5)
X=0.550 (X 2.0)
X=0.650 (X 2.0)
X=0.750 (X 2.0)
$F_2(x,Q^2)$
1
10^{-1}
1
10
10^2
10^3
Q^2 (GeV^2)

Fig. 1.b

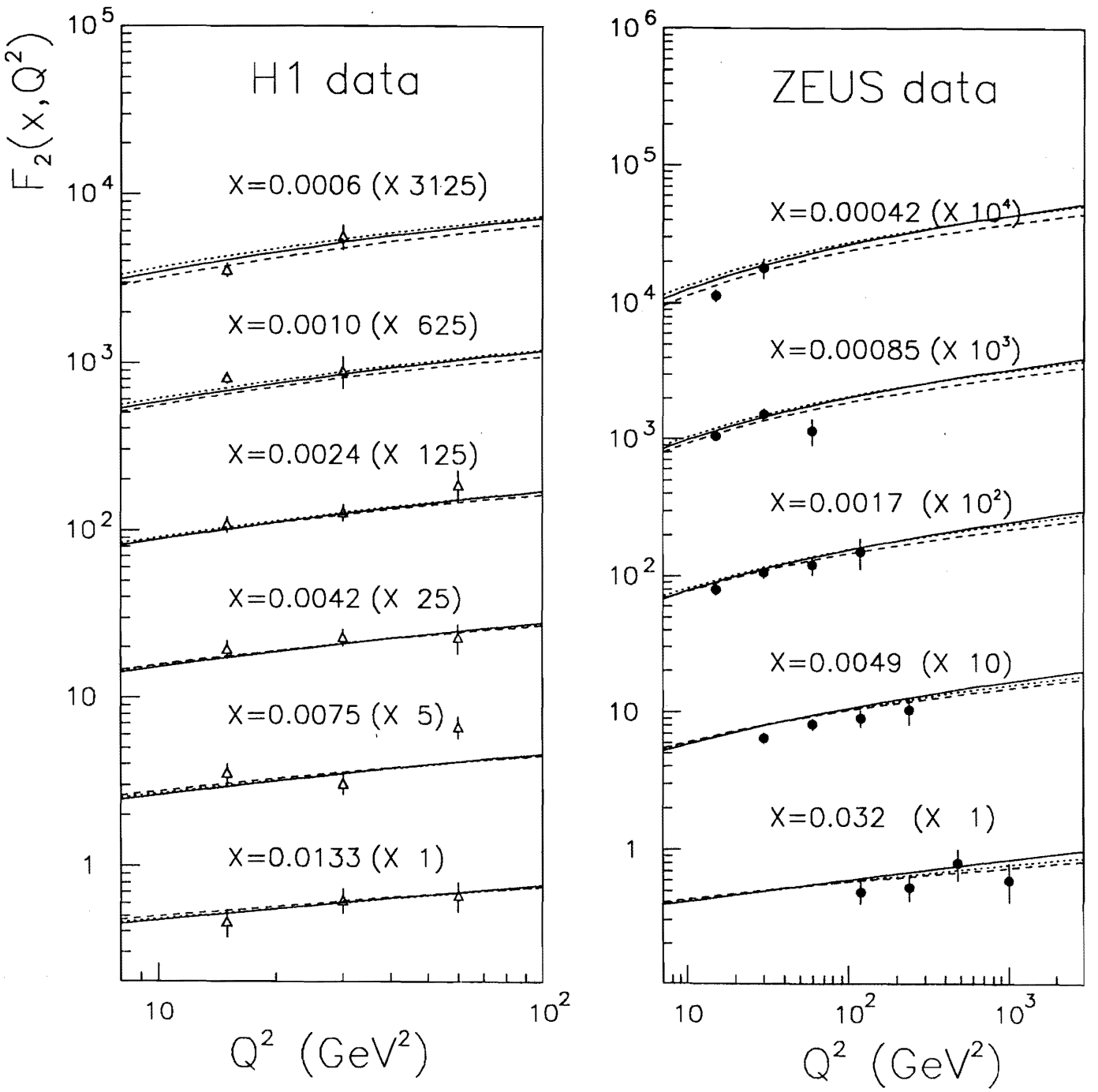
H1 data
ZEUS data
$F_2(x,Q^2)$
X=0.0006 (X 3125)
X=0.0010 (X 625)
X=0.0024 (X 125)
X=0.0042 (X 25)
X=0.0075 (X 5)
X=0.0133 (X 1)
X=0.00042 (X 10^4)
X=0.00085 (X 10^3)
X=0.0017 (X 10^2)
X=0.0049 (X 10)
X=0.032 (X 1)
Q^2 (GeV^2)
Q^2 (GeV^2)

Fig. 2

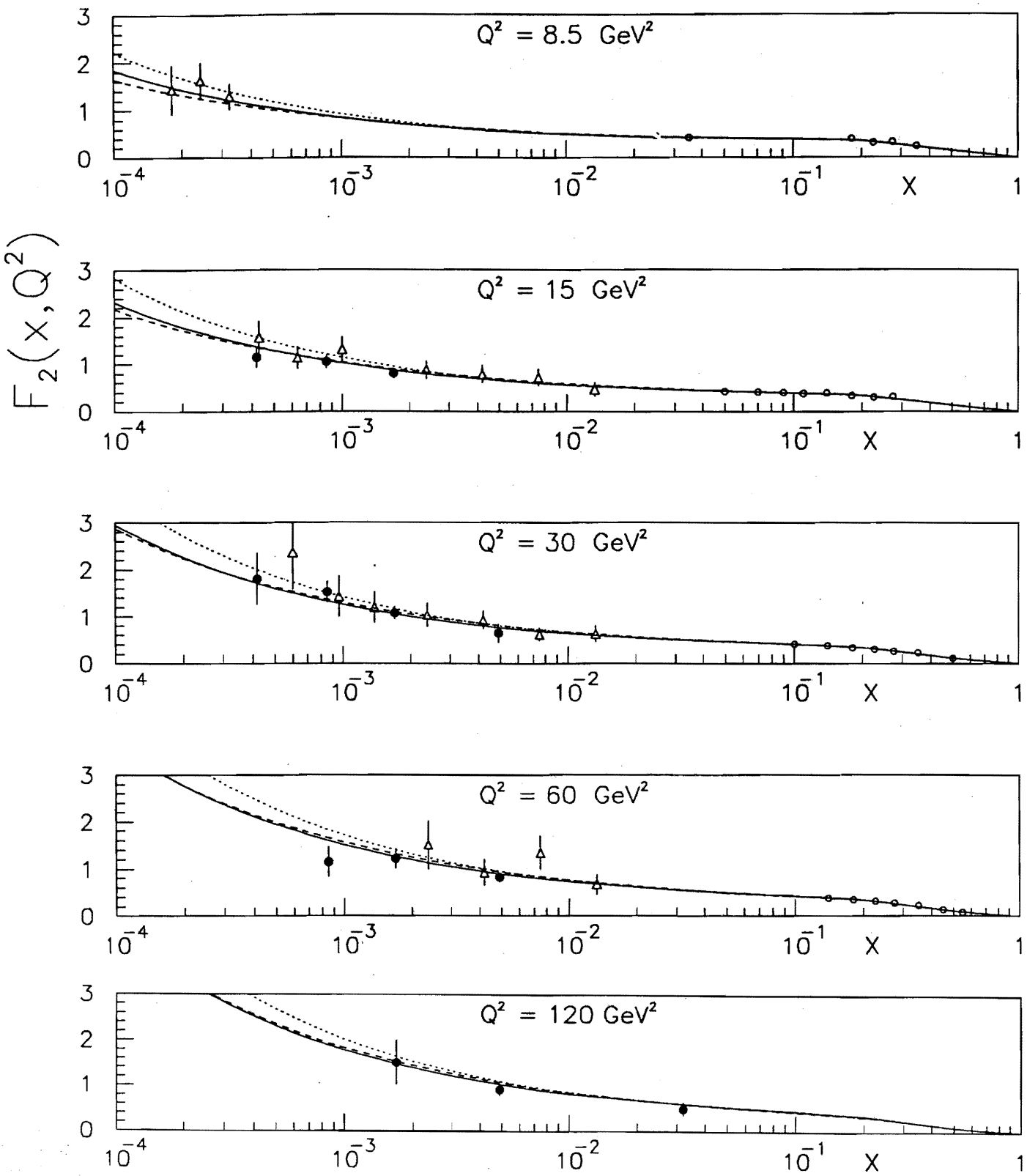

Fig. 3

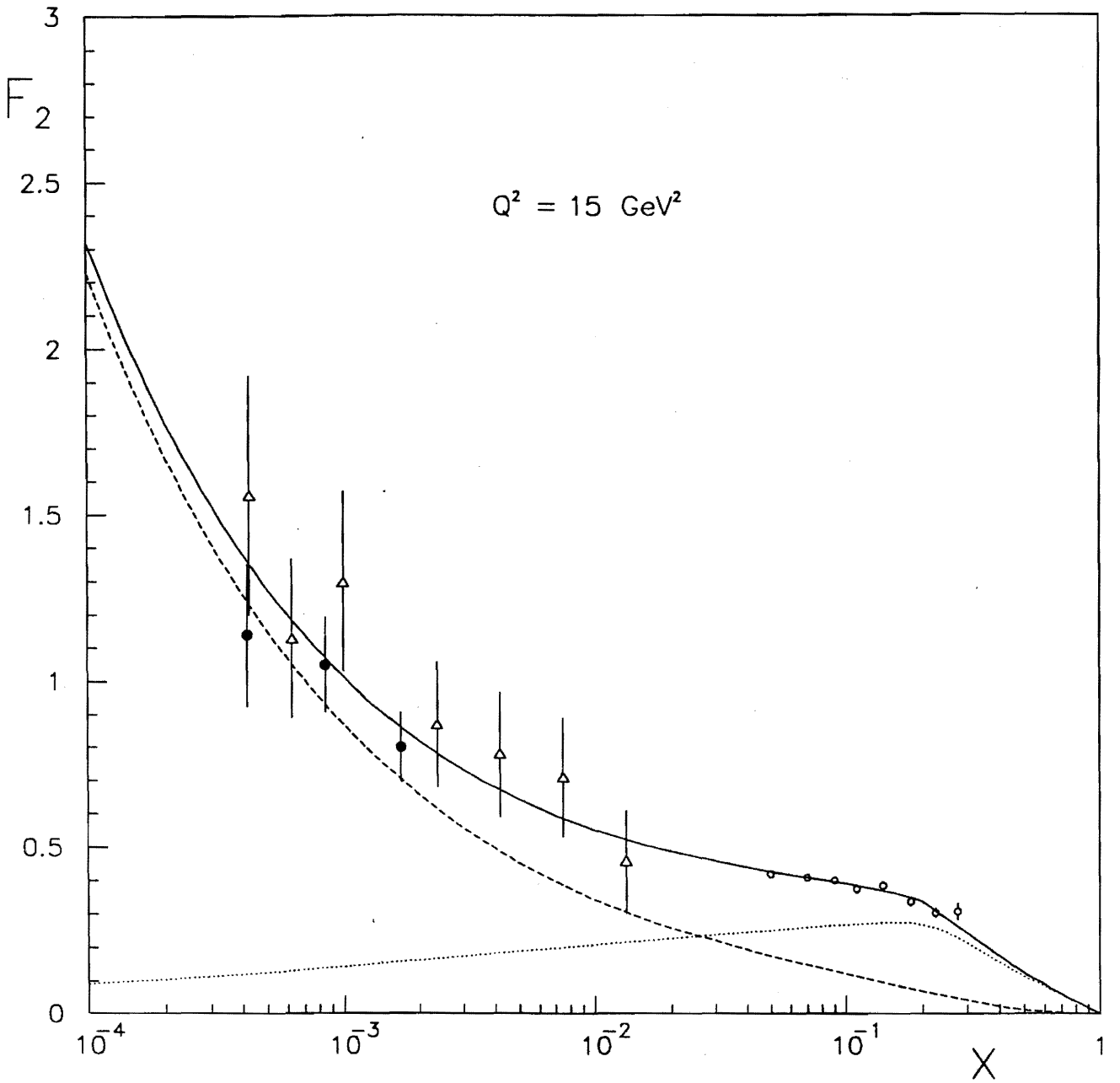

Fig. 4

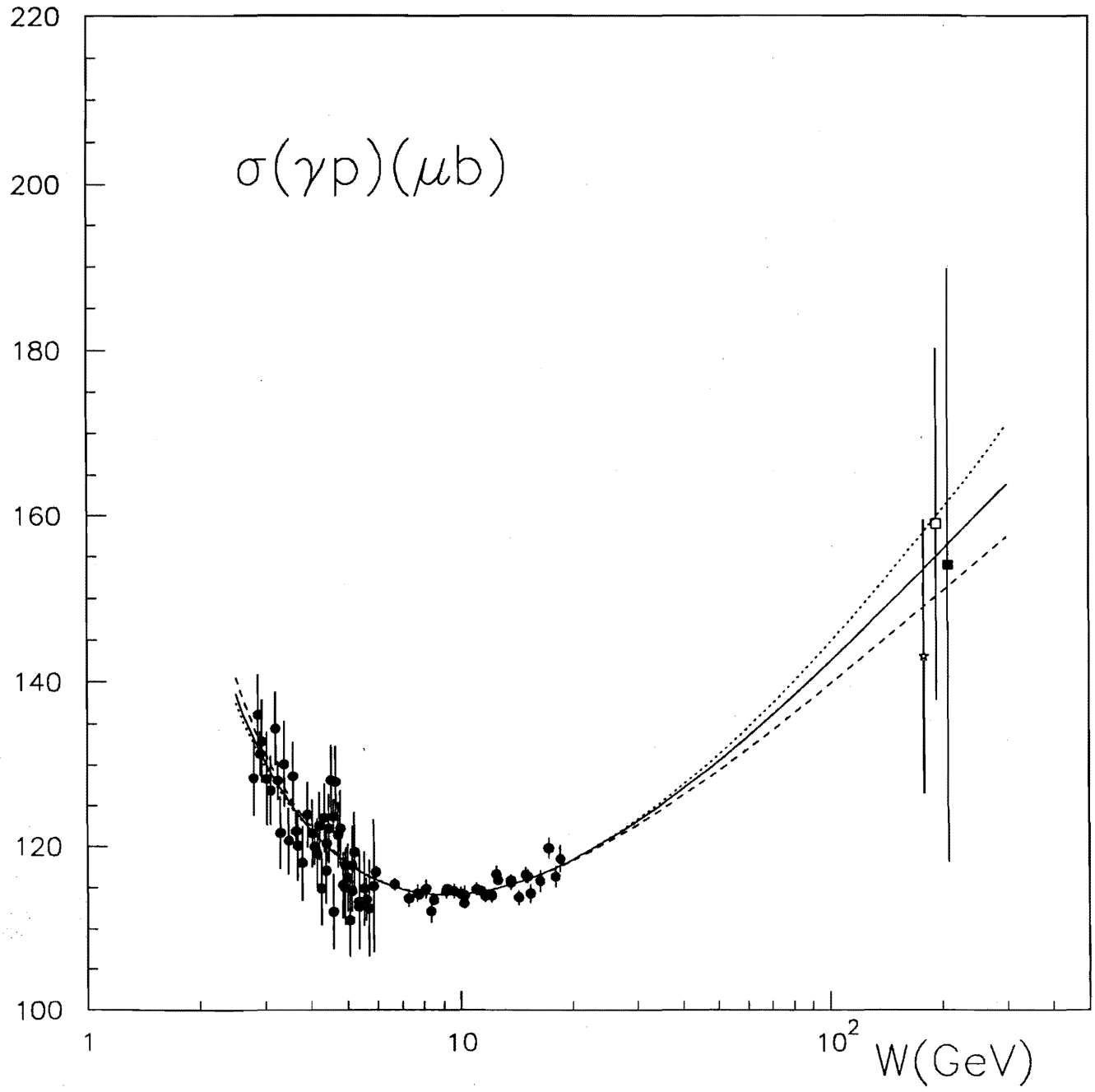

Fig. 5

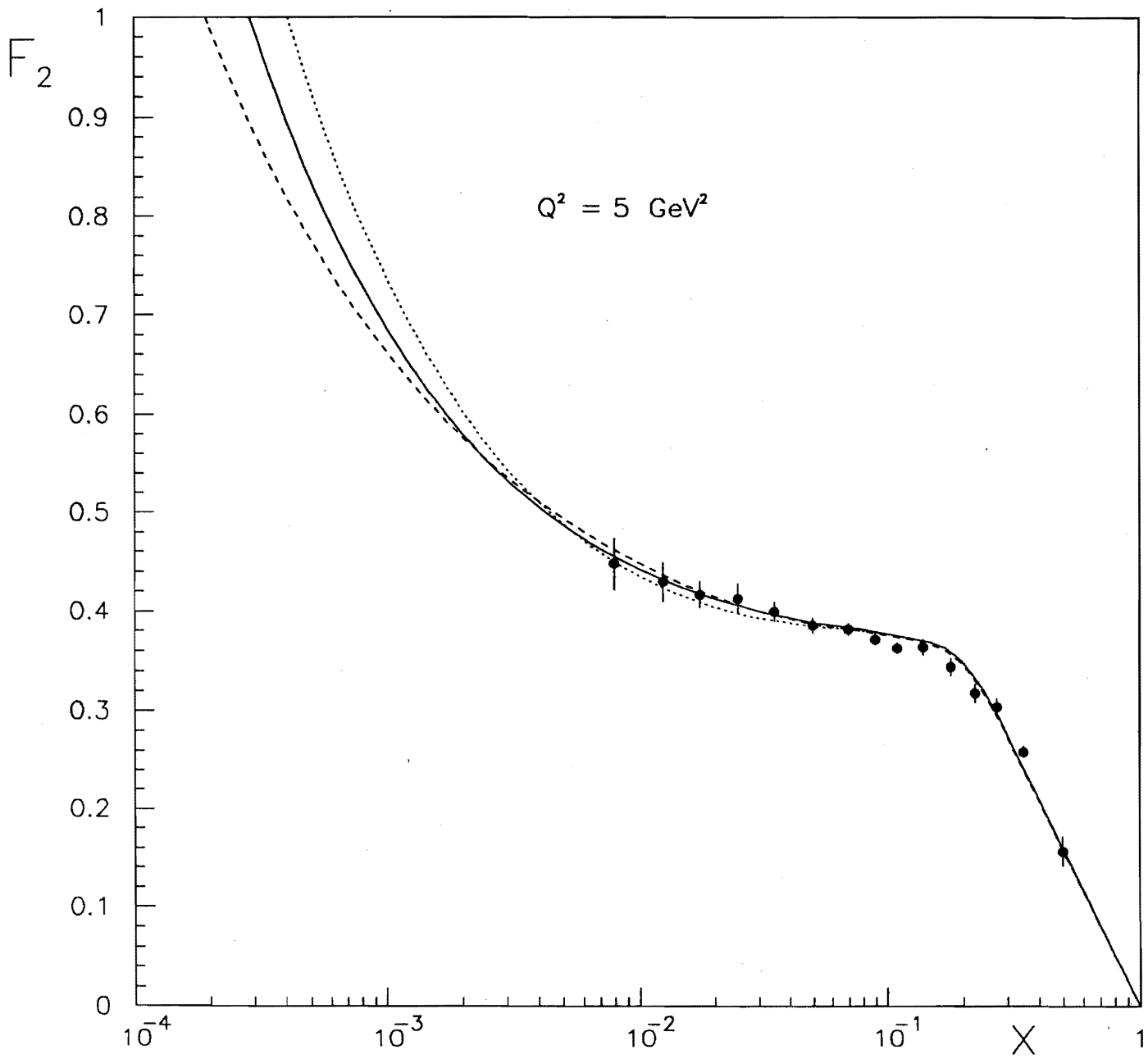

Fig. 6